

Rapid Measurement of Antioxidant Activity and γ -Aminobutyric Acid Content of Chinese Rice Wine by Fourier-Transform Near Infrared Spectroscopy

Zhengzong Wu · Enbo Xu · Jie Long · Fang Wang ·
Xueming Xu · Zhengyu Jin · Aiquan Jiao

Received: 21 December 2014 / Accepted: 2 March 2015 / Published online: 19 March 2015
© Springer Science+Business Media New York 2015

Abstract In this study, Fourier-transform near infrared (FT-NIR) spectroscopy in combination with chemometrics was utilized to determine the antioxidant capacity and γ -aminobutyric acid (GABA) content of Chinese rice wine (CRW). Interval partial least-squares (iPLS) and extreme learning machine (ELM) were used to improve the performances of partial least-squares (PLS) models. In total, four different calibration models, namely PLS, iPLS, ELM, and ELM models based on the subintervals selected by iPLS (iELM), were developed in this study. It was observed that the performances of models based on the efficient spectra intervals selected by iPLS were much better than those based on the full spectrum. In addition, nonlinear models were superior to linear models. After systemically comparison and discussion, it was found that for all of the four parameters determined, iELM model achieved the best result with excellent prediction precision. The coefficient of determination for the prediction set (R^2 (pre)), and the residual predictive deviation for the prediction set were 0.932 and 4.07 for 1,1-diphenyl-2-picrylhydrazyl assay, 0.970 and 6.21 for 2,2-azino-bis-(3-ethylbenzothiazoline-6-sulfonic acid) diammonium salt assay, 0.974 and 6.29 for total reducing antioxidant power assay and 0.952 and 4.75 for GABA, respectively. The overall results demonstrated that FT-NIR combined with efficient variable selection algorithm and nonlinear regression tool could be used as a rapid

alternative method for the prediction of the antioxidant capacity and GABA content of Chinese rice wine.

Keywords Chinese rice wine · Antioxidant capacity · γ -Aminobutyric acid · Extreme learning machine · Fourier-transform near infrared spectroscopy

Introduction

Chinese rice wine (CRW), also called as yellow wine, is a traditional Chinese alcoholic beverage fermented from glutinous rice with wheat Qu (as a source of saccharification enzymes) and yeast (*Saccharomyces cerevisiae*). It is one of the most popular alcoholic beverages in China and other Asian countries with an annual consumption of more than 2 million kiloliters (Xu et al. 2014). Due to the high contents of amino acids, proteins, oligosaccharides, vitamins, and mineral elements, CRW is also widely known for its health care function (Li et al. 2013). CRW has been claimed to have beneficial effects on the prevention of cancer, cardiovascular disease, atherosclerosis, diabetes, and aging (Que et al. 2006a). It is generally known that one of the key development steps of these chronic diseases is the oxidation process, which is mainly caused by the reactive oxygen species (ROS) and reactive nitrogen species (RNS), including free radicals such as superoxide anion radicals, hydroxyl radicals, and non-free radical species such as H_2O_2 and singlet oxygen (Zhang et al. 2013; Schonbichler et al. 2014). Thus, it is hypothesized that anti-disease effects of CRW are related with the antioxidant properties (Que et al. 2006b), in consideration of the fact that the strong antioxidant properties of CRW have been proved in several researches (Que et al. 2006a, b). Recent studies have also shown that there is a large amount of γ -aminobutyric acid (GABA) in CRW. GABA, catalyzed from glutamic acid by

Z. Wu · E. Xu · J. Long · F. Wang · X. Xu · Z. Jin · A. Jiao (✉)
The State Key Laboratory of Food Science and Technology,
School of Food Science and Technology, Jiangnan University,
1800 Lihu Road, Wuxi 214122, China
e-mail: jjiaoq@jiangnan.edu.cn

Z. Wu · E. Xu · J. Long · F. Wang · Z. Jin (✉) · A. Jiao
Synergetic Innovation Center of Food Safety and Nutrition,
Jiangnan University, 1800 Lihu Road, Wuxi 214122, China
e-mail: jinlab2008@yahoo.com

glutamic acid decarboxylase, is the most important inhibiting neurotransmitter in the brain with numerous health effects, such as increasing dopaminergic neuronal function, easing anxiety, and detoxification (Haugstad et al. 1997; Joye et al. 2011; DeFeudis 1983). Due to the increasing recognized functionality and health benefits of Chinese rice wine, antioxidant activity and γ -aminobutyric acid content have become two of the most important indicators of CRW quality. The determination of total antioxidant activity is generally based on the wet chemistry methods. For the analysis of antioxidant activity, several methods such as ferric ion reducing antioxidant power (FRAP) assay, 2,2'-diphenyl-picrylhydrazyl (DPPH) assay, and 2,2'-azino-bis-(3-ethylbenzothiazoline-6-sulfonic acid) diammonium salt (ABTS) assay are commonly used (Schonbichler et al. 2014). While for the measurement of γ -aminobutyric acid, the high-performance liquid chromatography (HPLC) method has been used for a long time (Kim et al. 2015). These traditional methods often show good precision, accuracy, and reliability. However, they are often time-consuming, labor intensive, subjective, and require expensive chemical reagents and equipments.

To overcome these drawbacks, infrared spectroscopy (IR) has emerged as a novel tool for quantitative measurements of these important indicators. IR technique, based on the molecules property to absorb infrared light and experience a wide variety of vibrational motions characteristic of the corresponding chemical compositions, is a fast, objective, and non-destructive method and has been gradually developed as an alternative to wet chemistry in the food industry and agriculture in the last few years (Jiang et al. 2012; Shen et al. 2011). In recent years, due to the distinct advantages including rapidity and easiness, several studies have been carried out on the application of mid infrared spectroscopy (MIR) technique in the determination of antioxidant activity in various wines (Lu et al. 2011; Versari et al. 2010). Nevertheless, few studies have focused on the application of near infrared spectroscopy (NIR) technique in the rapid measurement of antioxidant activity of wines. The NIR region of the electromagnetic spectrum lies between the visible and infrared regions and spans the range of wavelengths between 4,000 and 12,500 cm^{-1} . This region contains information concerning the relative proportions of C–H, N–H, S–H, and O–H bonds which are the primary structural components of organic molecules. CRWs from different wineries contain different contents of various chemical components which associate with the antioxidant capacity of CRW. These differences between different samples from different wineries can be reasonably existed in near infrared spectra and provide the potential of predicting the total antioxidant capacity and GABA by NIR. NIR tends to detect broad and unspecific overtone and combination vibrations originating from anharmonicities and seems to have advantages for the determination of sum parameters such as antioxidant activity, in comparison with MIR, which detects basic vibrations and

has exhibits advantages for quantification of individual compounds in some studies (Schonbichler et al. 2014; Wu et al. 2015). In addition, to the best of our knowledge, the combination of IR and chemometrics has not been used for the determination of antioxidant activity and GABA content of CRW. Moreover, almost all the studies regarding the rapid determination of antioxidant activity using IR technique focus on the multivariate regression models based on the full spectrum (Silva et al. 2014; Machado et al. 2014), little research exists on the calibration model based on the selected spectral region. As for wine samples, strong water absorption and a large number of uninformative and redundant spectral variables which would inevitably weaken the performances of final models exist in NIR spectra (Wu et al. 2014). A large number of studies have proved the efficiency of the application of variable selection methods in improving the performance of the multivariate regression models. In this study, interval partial least-squares (iPLS) algorithm, a promising spectral variable selection method proposed by Norgaard et al. (2000), is used to eliminate the uncorrelated variables existing in the full spectrum and improve prediction accuracy of the regression model. Moreover, CRW is a complex mixture consisting of hundred of component substances present at different concentrations (Shen et al. 2012a), complex correlations between determined parameters (antioxidant activity and γ -aminobutyric acid content) and NIR spectra data may exist, and linear regression models may not present perfectly the relationship between the NIR spectra and chemical parameters in CRW samples. In these cases, methods for linear modeling of nonlinear surfaces are needed. Extreme learning machine (ELM), as a new fast learning algorithm, is not only extremely fast but also tends to reach the smallest training error and norm of weights, and has shown its good performance in regression applications as well as in large dataset (and/or multi-label) classification applications (Chen et al. 2012; Huang et al. 2010; Lan et al. 2010; Rong et al. 2008). It is used in this study to provide a better solution to the modeling problem.

The aim of this study is to develop calibration models using NIR combined with characteristic variable selection algorithm (iPLS) and non-linear algorithm (ELM) for the prediction of antioxidant capacity and γ -aminobutyric acid content of Chinese rice wine. This approach would be useful for the evaluation of antioxidant capacity and γ -aminobutyric acid content in the beverage and nutraceutical industry.

Materials and Methods

Reagents

Sodium phosphate, borax, sodium azide, methanol, acetonitrile, γ -aminobutyric acid, 1,1-diphenyl-2-picrylhydrazyl, and

2,2-azino-bis-(3-ethylbenzothiazoline-6-sulfonic acid) diammonium salt (ABTS) were purchased from Sigma-Aldrich (St. Louis, MO, USA). Potassium ferricyanide, disodium hydrogen phosphate, sodium dihydrogen phosphate, trichloroacetic acid, iron trichloride, and ascorbic acid (vitamin C) were obtained from Sinopharm Chemical Reagent Co., Ltd. (Shanghai, China). All reagents and solvents used were analytical or HPLC grade. Water was purified by means of Milli-Q from Millipore (Bedford, MA, USA).

Sample Preparation

To build robust and reliable calibrations models, rice wine samples from five most well-known rice wine wineries were used in this study. Among, 21 samples were from “Guyuelongshan” brand, 25 samples were from “Kuaijishan” brand, 23 samples were from “Shazhouyouhuang” brand, 28 samples were from “Minzuhong” brand, and 23 samples were from “Shikumen” brand. A total of 120 Chinese rice wine samples were prepared for spectral and chemical analysis in the experiment. Additionally, even for the same brand of Chinese rice wine, they were independent because of different manufacturing dates, types (according to total sugar content), and quality grades.

Reference Analysis

HPLC Determination of γ -Aminobutyric Acid Content

The GABA content was determined following partially modified methods of Fürst et al. (1990). It was carried out using an HPLC gradient system (Thermo Fisher Scientific Co., LTD, MA, USA) equipped with a C18 column (6 mm×150 mm, 5 μ m, Acclaim 120, Dionex, Sunnyvale, CA, USA) and a fluorescence detector (FLD, UltiMate 3000, Thermo Fisher Scientific Co., LTD, MA, USA) detector. The sample was measured under an excitation wavelength of 335 nm and fluorescent wavelength of 390 nm. Binary eluents (mobile phase A containing 10 mM sodium phosphate, 10 mM borax, 0.5 mM sodium azide at pH 8.2, and mobile phase B containing acetonitrile, methanol, and distilled water at 45, 45, and 10 %, respectively) were used with a gradient program: 0–12 min, 10 % B; 12–13 min, 10–30 % B; 13–17 min, 30–90 % B; 17–20 min, 90–100 % B. The flow rate was 1.2 mL/min. The GABA concentration of each sample was determined using the standard curve.

Determination of Antioxidant Activity

1,1-Diphenyl-2-picrylhydrazyl Assay Reference analysis for DPPH assays was in accordance with the method described by Silva et al. (2014) with slight modifications. Briefly, a standard solution of DPPH 24 mg/L was prepared in

methanol. Wine sample (100 μ L) was mixed with 2 mL of DPPH solution, and the absorbance was measured immediately at 517 nm against a methanol blank with a UV–Vis spectrophotometer (TU-1900, Purkinje General Corporation, Beijing, China). After 30 min at room temperature, the absorbance was read again. The percent inhibition of DPPH radical caused by a wine sample was determined according to the following formula: $(A_{C(0)} - A_{A(t)}) / A_{C(0)} \times 100$, where $A_{C(0)}$ is the absorbance of the sample at $t=0$ min and $A_{A(t)}$ is the absorbance of sample at $t=30$ min. All samples were analyzed in triplicate.

2,2-Azino-bis-(3-ethylbenzothiazoline-6-sulfonic acid) Diammonium Salt Assay The ABTS assay was performed according to the method reported by Ozgen et al. with slight modifications (Ozgen et al. 2006). For the assay, ABTS⁺ radical was prepared by mixing an ABTS stock solution (7 mM in water) with 2.45 mM potassium persulfate. This mixture was allowed to stand for 12–16 h at room temperature in the dark until reaching a stable oxidative state. The ABTS⁺ solution was diluted with 20 mM sodium acetate buffer (pH 4.5) to an absorbance of 0.70 ± 0.01 at 734 nm. The reaction was started by the addition of 200 μ L of rice wine samples to 2 mL of the diluted ABTS⁺ solution. ABTS⁺ bleaching was monitored at 734 nm and 25 °C for at least 30 min, and the percentage of discoloration after 15 min was used as the measure of antioxidant activity. The ABTS⁺ bleaching was proportional to the concentration of the sample added to the medium. The antioxidant activity of CRW was calculated as vitamin C equivalents antioxidant activity (VCEAC) and was expressed as milligram of vitamin C equivalents per liter of rice wine sample. All measurements were performed in triplicate. A standard curve of the percentage of ABTS⁺ inhibition in function of vitamin C concentration (0.00–100.00 mg/L) was used for the calculations.

Total Reducing Antioxidant Power Assay The assay was performed according to the methods reported by Oyaizu (1986). Based on the preliminary experiment, 1 mL of each CRW sample was diluted fivefold with distilled water; then 1 mL of the diluent was mixed with 2.5 mL of phosphate buffer (0.2 M, pH 6.6) and 2.5 mL of potassium ferricyanide solution (10 g/L). The mixture was incubated in a water bath at 50 °C for 20 min. Then, 2.5 mL of trichloroacetic acid (TCA) solution (100 g/L) was added, and the mixture was then centrifuged at 3,000×g for 10 min. Of the upper layer, 2.5 mL was combined with 2.5 mL of distilled water and 0.5 mL of a ferric chloride solution (1 g/L). In this reaction, $K_3Fe(CN)_6$ was reduced by the sample, and $K_4Fe(CN)_6$ was formed, which in turn was reacted with Fe^{3+} ; then Prussian blue was formed, and a commercial spectrophotometer TU-1900 (Purkinje General Corporation, Beijing, China) was used to detect the absorbance at 700 nm of the reacted solution in a 1-cm-thick

quartz cell. Higher absorbance indicates greater total reducing antioxidant power (TRAP), which represents higher antioxidant activity. The ferric reducing antioxidant power of the CRW samples was determined in triplicate and expressed as milligram of vitamin C equivalents (mg VCEAC/L).

FT-NIR Instrumentation and Spectral Collection

An Antaris II near-infrared spectrometer (Thermo Electron Corp., Madison, WI, USA) in combination with the software package RESULT (v. 8.0, Thermo Electron Corp., Madison, WI, USA) was utilized to obtain the NIR spectra. The spectral data were collected at controlled temperature (25 ± 1 °C) and the spectra were recorded for each sample from 10,000 to 4,000 cm^{-1} by averaging 16 scans for each sample with a spectral resolution of 8 cm^{-1} . Rice wine samples were measured in a quartz cuvette with a 1-mm optical path length that was a standard accessory from this spectrophotometer. Water was used to clean the cuvette and dried with the help of a soft tissue paper to avoid contamination over samples. Spectra were recorded in triplicate for each sample and the mean was used in the next analysis.

Data Analysis

Before forming multivariate regression models, to mitigate background information and noises except sample information exist in the raw spectra collected from NIR measurements, eight pretreatment methods were employed to preprocess the raw spectra, i.e., Savitzky–Golay (SG) smoothing (window size of 9 points, two-order polynomial), multiplicative scattering correction (MSC), standard normal variate (SNV), the first derivative (D1), the second derivative (D2), baseline (BL), moving average smoothing (MA), and detrending (DT). For MSC, full MSC function was adopted in this study. While for D1 and D2, smoothing points from 3 to 11 and the polynomial orders of 1 and 2 were attempted. The optimal pre-processing method is achieved in accordance with the lowest root mean square error of cross validation (RMSECV) value based on partial least-squares (PLS) models, considering that PLS is the most widely used regression methods.

In order to reduce colinearity and redundancy of NIR spectra and to build more robust calibration models, iPLS algorithm was used to select efficient wavelengths in this study.

Calibration models between NIR spectra and the reference measurements were developed using PLS and ELM regression algorithms with leave-one-out cross validation (LOOCV). Cross validation estimated the prediction error by splitting all samples into two groups. One group was reserved for validation (only one observation in this group), and the others were used for calibration. The process was repeated until all the samples had been used once in the validation

set. This verification approach is useful because it does not waste data (all samples are involved in the development of the model), and it is more suited to a small amount of samples (de Oliveira et al. 2014). The optimum number of factors in the PLS regression models is determined by the lowest number of factors that yields the minimum value of the prediction residual error sum of squares (PRESS) in the cross validation to avoid over fitting in the models. Outlier detection was also applied before the development of calibration models by using the leverage criteria and the student residuals

To evaluate the model fit to the data in the calibration set, the coefficient of determination for the calibration set (R^2 (cal)) and RMSECV were used in this study and were calculated according to Eqs. (1–2):

$$R^2(\text{cal}) = 1 - \frac{\sum_{i=1}^n (\hat{y}_{ci} - y_{ci})^2}{\sum_{i=1}^n (\hat{y}_{ci} - \bar{y}_c)^2} \quad (1)$$

$$\text{RMSECV} = \sqrt{\frac{\sum_{i=1}^{n_c} (\hat{y}_{ci} - y_{ci})^2}{n_c}} \quad (2)$$

where n_c is the number of samples in the calibration set, y_{ci} is the reference measurement value obtained from chemical methods for the sample i , \hat{y}_{ci} is the predicted value by NIR spectra for sample i , and \bar{y}_c is the mean of the reference measurement results for all samples in the calibration set.

The prediction accuracy of the calibration model was tested by the coefficient of determination for the prediction set (R^2 (pre)) and root mean square error of prediction (RMSEP), which were calculated by Eqs. (3–4):

$$R^2(\text{pre}) = 1 - \frac{\sum_{i=1}^n (\hat{y}_{pi} - y_{pi})^2}{\sum_{i=1}^n (\hat{y}_{pi} - \bar{y}_p)^2} \quad (3)$$

$$\text{RMSEP} = \sqrt{\frac{\sum_{i=1}^{n_p} (\hat{y}_{pi} - y_{pi})^2}{n_p}} \quad (4)$$

where n_p is the number of samples in the prediction set, y_{pi} is the reference measurement value obtained from chemical methods for the sample i , \hat{y}_{pi} is the predicted value by NIR spectra for sample i by the model developed when the i th sample is left out, and \bar{y}_p is the mean of the reference measurement results for all samples in the prediction set.

Additionally, residual predictive deviation (RPD), which is defined as the ratio of the standard deviation (SD) of the reference data to the standard error of cross validation or the standard error of prediction, was also used in this study to standardize the predictive accuracy. Generally, if an RPD

value is greater than 3, the model can be used for analytical purposes with excellent prediction accuracy. An RPD value between 2 and 3 is considered that this model has a good precision. Whereas, if the value of RPD is lower than 2, the model is considered insufficient for prediction purposes (Shen et al. 2011). The higher the RPD value, the greater the ability of the model to predict the chemical compositions accurately for external samples outside the calibration set.

The spectral pretreatments and PLS were implemented in the commercial chemometric software The Unscrambler (v 10.2; CAMO Software AS, Oslo, Norway). The ELM models were implemented in Matlab R2010a (MathWorks, Natick, USA) under Windows XP. The iPLS algorithm in the work was developed by Nørgaard et al. and the iPLS Matlab codes were downloaded from <http://www.models.kvl.dk/> for free of charge, while the Matlab codes of ELM algorithm were downloaded from http://www.ntu.edu.sg/home/egbhuang/ELM_Codes.htm for free of charge.

Results and Discussions

GABA Content and Total Antioxidant Capacities in Chinese Rice Wine

The mean, standard deviation, range, and coefficient of variation of Chinese rice wine data set for DPPH, ABTS, TRAP, and GABA content are summarized in Table 1. Results for the four parameters measured in this study show a wide range of values, which may be due to differences in the manufacture practices and composition of the raw materials. The GABA contents in Chinese rice wines varied from 146.3 to 324.7 mg/L, with a mean value of 228.3 mg/L. For the evaluation of the total

antioxidant capacity of CRW samples, three different kinds of antioxidant assays, namely DPPH, ABTS, and TRAP, were applied in this study. TRAP assays measured the capacity of reducing metals (ferric to ferrous iron). TRAP values ranged from 21.3 to 112.8 mg VCEAC/L with a mean value of 52.9 mg VCEAC/L. For the DPPH assay, the higher the percentage inhibition, the higher the antioxidant capacity for the radical the CRW sample has. In this study, DPPH inhibition changed from 20.3 to 66.7 % with an average value of 40.0 %. ABTS assays is originally introduced as TEAC assay by Miller et al. and modified by Re et al. (Schonbichler et al. 2014). In the present study, ABTS assays had also a wide range of variation between 23.7 and 45.4 mg VCEAC/L with an average value of 35.8 mg VCEAC/L. These important differences among the samples are beneficial for the development of robust calibration models. In addition, results also show that Chinese rice wines have a significant antioxidant capacity due to their chemical composition, regardless of the brands and the manufacture dates of CRW used in this study, which was also reported by other researchers (Que et al. 2006b). Chinese rice wine is widely known for its healthy function and is honored as “liquid cake,” due to its high contents of various amino acids, proteins, polyphenols, Maillard reaction products, GABA, oligosaccharides, vitamins, and mineral elements (Li et al. 2013). These functional components play important roles in the forming of the strong antioxidant capacity of Chinese rice wine, which had been proved by many researchers (Que et al. 2006b; Pang and Zhang 2011; Xie et al. 2005; Ye et al. 2006; Fan and Qiao 2000; Peng et al. 2012; Tan et al. 2014). Thus, the antioxidant capacity of CRW is the result of many variables including redox potentials of the compounds present in the matrix, cumulative and synergistic interaction, and nature of the oxidizing substrate. Furthermore, obvious differences among the results of three different antioxidant methods used in this study were observed. Among the three assays, the TRAP assay obtained the highest values, whereas the ABTS assay demonstrated the lowest value. The DPPH assay gave an intermediate result. The trend observed here for results of the three assays for total antioxidant capacity determination was also observed by Schonbichler et al. (2014). The variations of total antioxidant capacity determined by different chemical assays also validated the problems of using one-dimensional method to evaluate multifunctional food and biological antioxidants, suggesting the necessary of efficient method to solve this problem. The contents of GABA of CRW samples obtained are generally in agreement with values reported in the previous studies (Liu et al. 2014; Xie et al. 2005).

FT-NIR Spectral Features of Chinese Rice Wine

Fourier-transform near infrared (FT-NIR) spectra of CRW samples for the whole sample set are presented in Fig. 1a. The absorbance in the NIR is comparable with those reported in the literatures (Yu et al. 2007; Shen et al. 2012b). As could

Table 1 Descriptive statistics for the chemical parameters used for the development of FT-NIR calibration and prediction models

	Mean	SD ^a	Range	CV ^b
Calibration (<i>n</i> =90)				
DPPH (%)	40.2	11.5	20.3–66.7	28.6
ABTS (mg VCEAC/L)	35.9	5.0	23.7–45.4	14.0
TRAP (mg VCEAC/L)	53.3	24.7	21.3–112.8	46.4
GABA(mg/L)	228.8	43.5	146.3–324.7	19.0
Prediction (<i>n</i> =30)				
DPPH (%)	39.2	11.1	21.1–64.5	28.2
ABTS (mg VCEAC/L)	35.5	5.1	23.7–45.0	14.3
TRAP (mg VCEAC/L)	51.6	23.4	22.1–106.4	45.4
GABA(mg/L)	226.7	43.0	152.1–304.2	19.0

^a Standard deviation

^b Coefficient of variation [$\{SD / \text{mean}\} \times 100$]

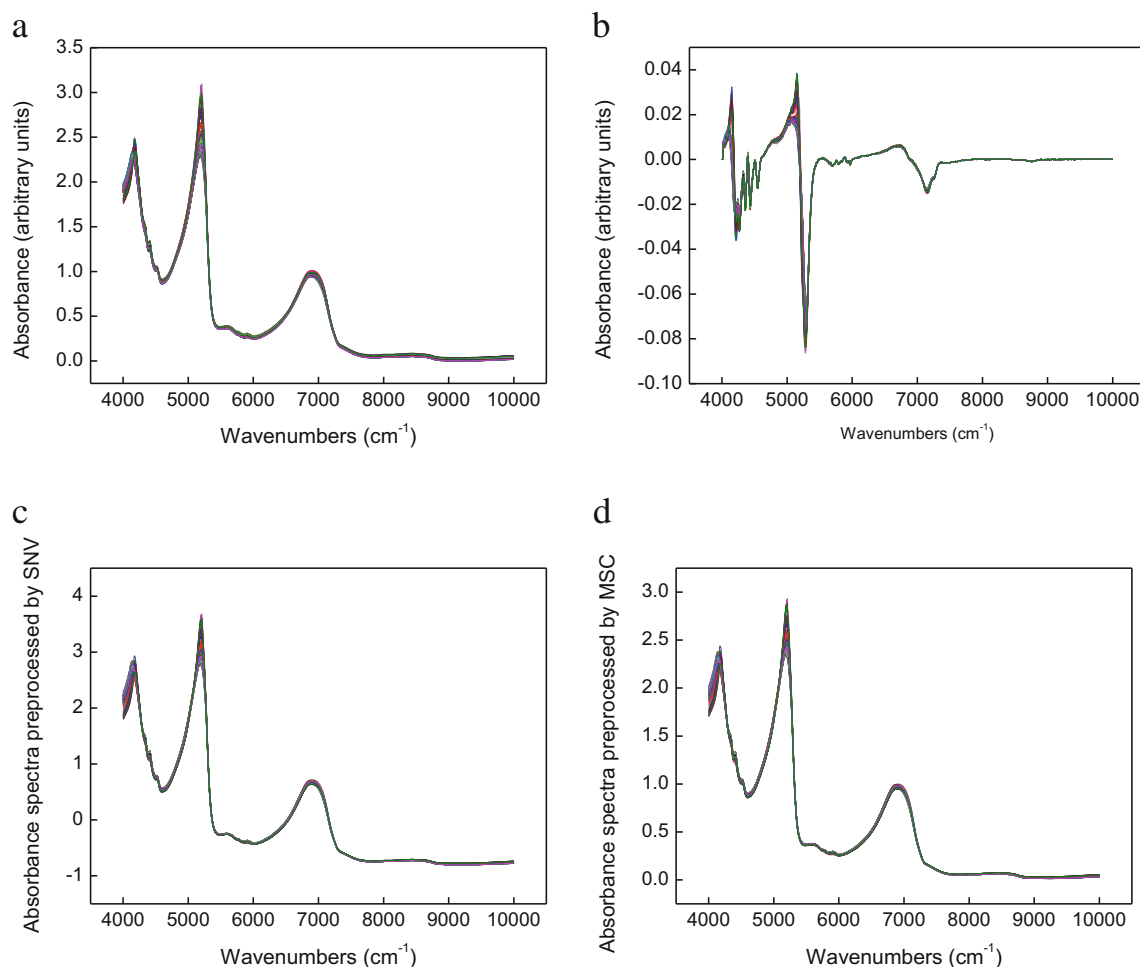


Fig. 1 Raw spectra (a), D1 (b), SNV (c), and MSC (d) preprocessed FT-NIR spectra of all CRW samples

be seen in the figure, the main features of the spectra are at around 4,155, 6,896, 5,000–5,250, 4,453, and 4,338 cm^{-1} . These absorption bands are more evident in the first derivative plot (Fig. 1b). The three dominating absorption peaks that belonged to water (the most abundant component in wine samples) were observed at around 4,155 cm^{-1} corresponded to the combination of stretch and deformation of the CH_2 group (Zhang et al. 2014), at around 6,896 cm^{-1} related to the first O–H overtone in water or carbohydrate, and at 5,000–5,250 cm^{-1} related to the combination of stretch and deformation of the O–H group (Shen et al. 2010b). The small absorption band at 5,108 cm^{-1} was related to O–H stretch and C=O second overtone combinations, that at 5,917 cm^{-1} might be related to the $-\text{CH}_3$ stretch first overtone or C–H groups in aromatic compounds, and that at 5,586 cm^{-1} , associated with the absorption of $-\text{CH}_3$ and C–H stretching and O–H from sucrose, fructose, and glucose (Niu et al. 2008). Two characteristic broad absorption bands which belong to ethanol were observed at around 4,453 cm^{-1} , assigned to C–H combinations and O–H stretch overtones, and at around 4,338 cm^{-1} , explained by the combination of stretch and deformation of

C–H from the $-\text{CH}_2$ group (Shen et al. 2010a). According to the literature (Niu et al. 2008), the smaller absorption bands at 8,438 cm^{-1} might due to the combination of the first overtone of the O–H stretching and bending from water.

Quantitative Analysis

All 120 samples were divided into two subsets. The first subset was called calibration set to be used for building model, while the other one was called prediction set to be used for testing the robustness of the model. To avoid bias in subset division, the division was made using the Kennard-Stone (KS) algorithm, which proposed a sequential method that should cover the experimental region uniformly. The KS algorithm ensures that the prediction samples are in the experimental space of the calibration set, minimizing the extrapolation when the prediction samples are predicted. The detailed procedure consists of selecting the first two samples with the largest Euclidean distance for the calibration set. Then, from the rest of all possible samples, the one that is most distant from those already selected was chosen, and it was included in

the calibration set. The selection process was repeated until the desired number of samples for the calibration set was reached. The remaining samples were used to create the prediction set. Finally, the calibration set contained 90 samples and the prediction set contained 30 samples. The descriptive statistics for the four parameters measured in this study are shown in Table 1. It is observed that the ranges of four reference measurements results of DPPH, ABTS, TRAP, and GABA in the calibration set cover the entire range in the prediction set, and their standards deviations in the calibration and prediction sets are no significant differences. Thus, their distributions of the samples are appropriate in the calibration and prediction sets.

Spectral Data Processing

Table 2 shows the results of PLS models with full cross validation using different processing methods. Some of the pretreatment methods increased the performances of the PLS model, while the prediction accuracy decreased by using some other preprocessing methods. This might due to the fact that on one hand appropriate pretreatments may eliminate some unwanted background information, on the other hand, significant noise might also generated. It is observed that for all of the four parameters used in this study, good performances are obtained, with the best R^2 of each parameter over 0.900, indicating excellent calibration models were obtained. The optimal preprocessing methods for the four parameters are prominently shown in italics. As shown in Table 2, for DPPH, ABTS, and TRAP, SNV achieved the best results with the lowest RMSECV and the highest R^2 , whereas for GABA, the best processing method was MSC. Thus, NIR spectra preprocessed by SNV (for DPPH, ABTS, and TRAP) and MSC (for GABA) were applied for the following analysis. And the spectra preprocessed by SNV and MSC were shown in Fig. 1c and d, respectively.

Selection of Efficient Spectra Intervals

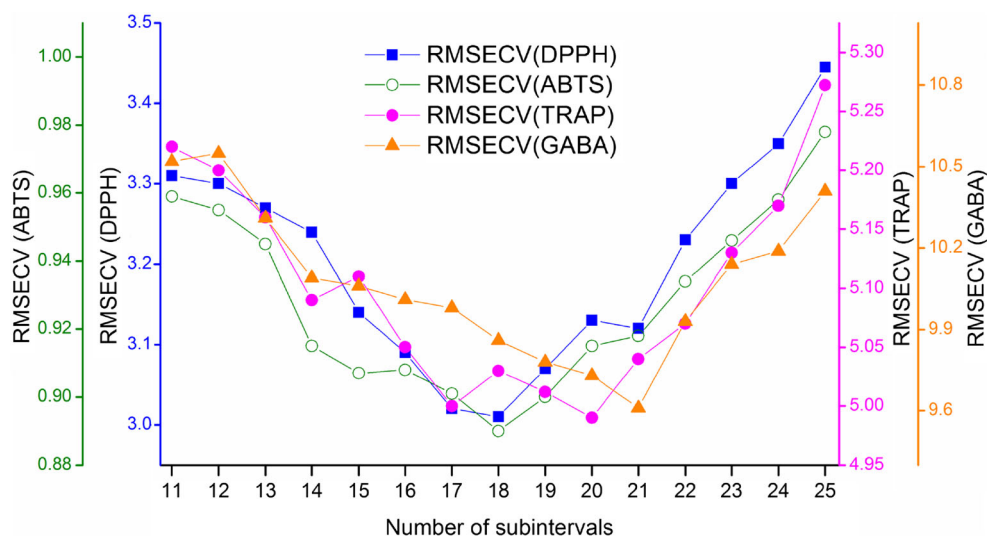
iPLS algorithm, a new type of graphically oriented local modeling procedure, is an interactive extension to PLS. The basic principle of this algorithm is as follows: first, the full data interval is subdivided into a number of smaller equidistant subintervals; second, PLS models for all spectral intervals were developed with adequate number of latent variables; finally, the RMSECV is calculated for each PLS model based on different subintervals. The subintervals with the lowest RMSECV are chosen to construct the optimal iPLS models.

By using iPLS algorithm, most of the redundant or uninformative variables that exist in NIR spectra can be removed. However, it has shown that, in some cases, the prediction precision of model would be inevitably weakened when inappropriate number of divided subintervals was applied in the research (Wu et al. 2015). Thus, the number of the divided subintervals was optimized in this work. The whole spectrum region was divided into 11–25 intervals, and then iPLS models based on different number of intervals divided were established. Results of the RMSECV values of the optimal iPLS models under different number of subintervals divided in this work for the four parameters studied were shown in Fig. 2. It was observed that for DPPH and ABTS, the lowest RMSECV was achieved when the full spectra were divided into 18 subintervals, while for TRAP, the number of subdivided spectral intervals was 20, for GABA, that was 21. Figure 3 shows the optimal subintervals selected by iPLS algorithm for the prediction of DPPH, ABTS, TRAP, and GABA. As could be seen in the figure, for TRAP, the optimal iPLS model (with the lowest RMSECV) was achieved when the second subinterval in the range of 4,601.32–4,898.31 cm^{-1} was used to establish PLS regression models; for GABA, the optimal iPLS model was achieved when the second subinterval in the range of 4,288.91–4,574.32 cm^{-1} was chosen to develop PLS models, while for DPPH and ABTS, the efficient spectral interval was the fourth subinterval in the range of 4,670.75–5,002.44 cm^{-1} .

Table 2 Results of PLS models using different pretreatments

Pretreatment	DPPH		ABTS		TRAP		GABA	
	R^2	RMSECV	R^2	RMSECV	R^2	RMSECV	R^2	RMSECV
Raw	0.872	3.58	0.918	1.07	0.934	4.99	0.883	12.60
SG	0.882	3.47	0.922	1.06	0.928	5.30	0.911	12.11
MSC	0.860	3.83	0.898	1.28	0.924	5.35	<i>0.924</i>	<i>11.66</i>
SNV	<i>0.903</i>	<i>3.32</i>	<i>0.927</i>	<i>1.01</i>	<i>0.943</i>	<i>4.55</i>	0.914	11.88
D1	0.891	3.40	0.903	1.20	0.918	5.52	0.882	12.90
D2	0.874	3.57	0.924	1.03	0.932	5.22	0.911	11.96
BL	0.889	3.44	0.912	1.10	0.933	5.10	0.920	11.72
MA	0.863	3.71	0.910	1.14	0.920	5.43	0.894	12.42
DT	0.869	3.66	0.914	1.08	0.931	5.22	0.903	12.25

Fig. 2 Results of the optimal iPLS models under different number of subintervals divided for DPPH, TRAP, ABTS, and GABA



Comparison of Different Kinds of Calibration Models

In this study, the selected wavenumbers were used inputs of PLS and ELM to build more robust calibration models. In total, four different regression models, namely PLS, iPLS, ELM, iPLS-based ELM (iELM), were constructed and their results were systemically compared and discussed. A summary of the results of four different multivariate regression models developed for each parameter was shown in Table 3.

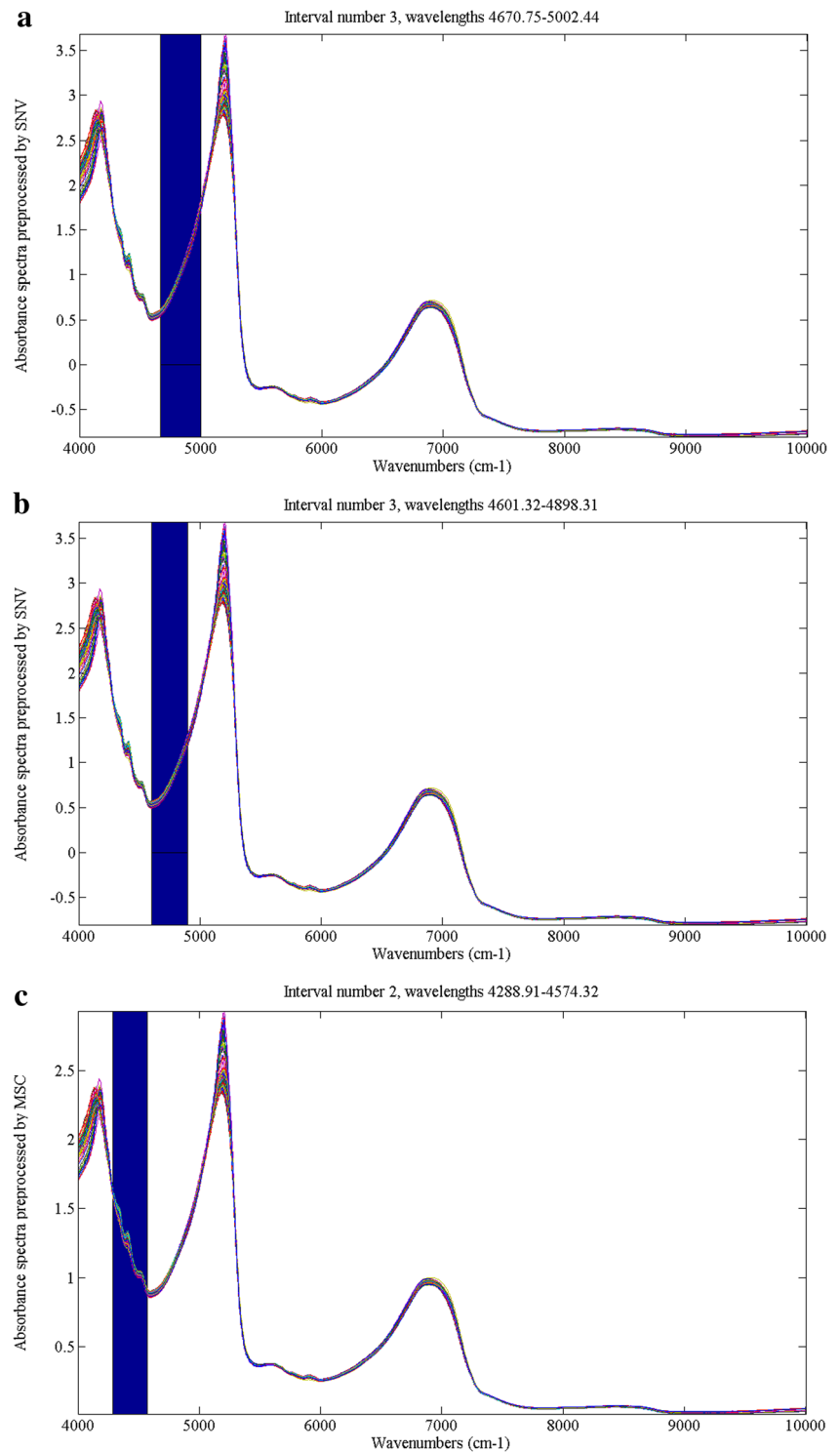
Results of PLS Models

Investigated from Table 3, good performances were obtained from the PLS models established in this study. In the calibration sets, the correlation coefficients of calibration (R^2 (cal)), RMSECV (%), and the RPD were of 0.903, 8.26, and 3.46, respectively, for DPPH; 0.927, 2.80, and 4.99, respectively, for ABTS; 0.943, 8.53, and 5.43, respectively, for TRAP; and 0.924, 5.10, and 3.73, respectively, for GABA. The R^2 of the four parameters were all higher than 0.900, while the RPD value obtained for these four parameters were all higher than 3. According to the criteria reported by other authors (Wu et al. 2015), the overall results indicated that FT-NIR could be used as a rapid method to determine the antioxidant capacity and GABA content of Chinese rice wine. It was remarkable that a relative high RMSECV (%) (or RMSEP (%)) and a relative low RMSECV (%) (or RMSEP (%)) were observed for TARP and ABTS, respectively, in comparison with that of DPPH and GABA. This may be due to that the RMSECV (RMSEP) value is related with the range of reference values. A wide range in chemical composition usually results in high RMSECV (RMSEP) values, and vice versa. It is in accordance with the statistics shown in Table 1, the widest range (or CV value) is observed for TARP while the narrowest range (or CV value) is observed for ABTS.

Results of iPLS Models

As could be seen in Table 3, iPLS model showed its robustness in comparison with PLS model based on full-spectral region, as all of the iPLS models developed for the four parameters based on the optimal subintervals performed much better than those models developed based on the full spectrum except TRAP. The classic calibration models are often constructed based on the full spectrum. However, a large number of unrelated and collinear spectral variables such as variables from the saturated absorption bands of O–H from water involve in the full spectrum, with which a worse prediction be obtained. Therefore, spectra variables selection is needed to improve the performance of the full spectrum model. The main force of iPLS algorithm is to provide an overall picture of the relevant information in different spectral subdivisions, thereby focusing on important spectral regions and removing interferences from other regions. It was found that the efficient intervals selected by iPLS for DPPH, ABTS, and TRAP were all at around 4,500–5,000 cm^{-1} , which related with the C–H stretch, O–H stretch, and its interaction with the aromatic ring (Schonbichler et al. 2014). According to the opinion of Que et al. (2006a), two phenolic compounds, namely syringic acid and (+)-catechin, contributed most to the total antioxidant capacity of CRW. The O–H group and aromatic ring were the main functional groups of the abovementioned two polyphenol. There were as high as five hydroxyl groups attached to two benzene rings in one syringic acid molecule and one O–H group and one benzene ring in one catechin molecule. Thus, the selected NIR regions well represent the contents of these two most important polyphenols in CRWs. While for GABA, the selected optimal interval was the second interval in the range of 4,288.91–4,574.32 cm^{-1} . The spectra in this region were assigned to the combinations of the first overtone of C=O stretch with fundamental N–H in plane bend and the first overtone of N–H in plane bend with fundamental C=O stretch

Fig. 3 The optimal subintervals selected by iPLS algorithm for the prediction of DPPH and ABTS (a), TRAP (b), and GABA (c)



(Zhang et al. 2014; Ouyang et al. 2012). To better understand the results got from iPLS, the regression coefficients for the optimal PLS models of the four parameters based on the full spectrum were also studied. As could be seen in Fig. 4, for DPPH, ABTS, and TRAP (Fig. 4a–c), a significant broad band was all observed at around 4,500–4,

800 cm^{-1} , indicating that spectral variables in this region contribute more than other variables in building robust models. For GABA (Fig. 4d), the main region with the highest regression coefficients was obtained in the spectral interval 4,300–4,500 cm^{-1} . Overall, the results got from the plots of regression coefficients accorded with the

Table 3 Comparison of results based on different regression models

Parameters	Model	Variables	Calibration				Prediction			
			R^2	RMSECV	RMSECV (%)	RPD	R^2	RMSEP	RMSEP (%)	RPD
DPPH	PLS	1,557	0.903	3.32	8.26	3.46	0.894	3.35	8.55	3.30
	iPLS	87	0.920	3.01	7.49	3.81	0.910	3.26	8.32	3.39
	ELM	1,660	0.924	2.84	7.06	4.04	0.914	3.15	8.03	3.52
	iELM	87	0.942	2.58	6.41	4.46	0.932	2.72	6.93	4.07
ABTS	PLS	1,557	0.927	1.01	2.80	4.99	0.924	1.03	2.89	4.94
	iPLS	87	0.941	0.89	2.46	5.67	0.932	0.96	2.71	5.27
	ELM	1,660	0.959	0.85	2.37	5.89	0.953	0.87	2.45	5.83
	iELM	87	0.972	0.79	2.19	6.39	0.970	0.82	2.30	6.21
TRAP	PLS	1,557	0.943	4.55	8.53	5.43	0.933	5.01	9.70	4.68
	iPLS	78	0.934	4.99	9.36	4.95	0.927	5.32	10.31	4.40
	ELM	1,660	0.963	3.90	7.32	6.33	0.961	4.21	8.17	5.56
	iELM	78	0.982	3.55	6.65	6.97	0.974	3.73	7.22	6.29
GABA	PLS	1,557	0.924	11.66	5.10	3.73	0.922	11.69	5.16	3.68
	iPLS	74	0.941	9.61	4.20	4.53	0.939	9.88	4.36	4.36
	ELM	1,660	0.938	10.02	4.38	4.34	0.933	10.57	4.66	4.07
	iELM	74	0.954	8.75	3.82	4.97	0.952	9.07	4.00	4.75

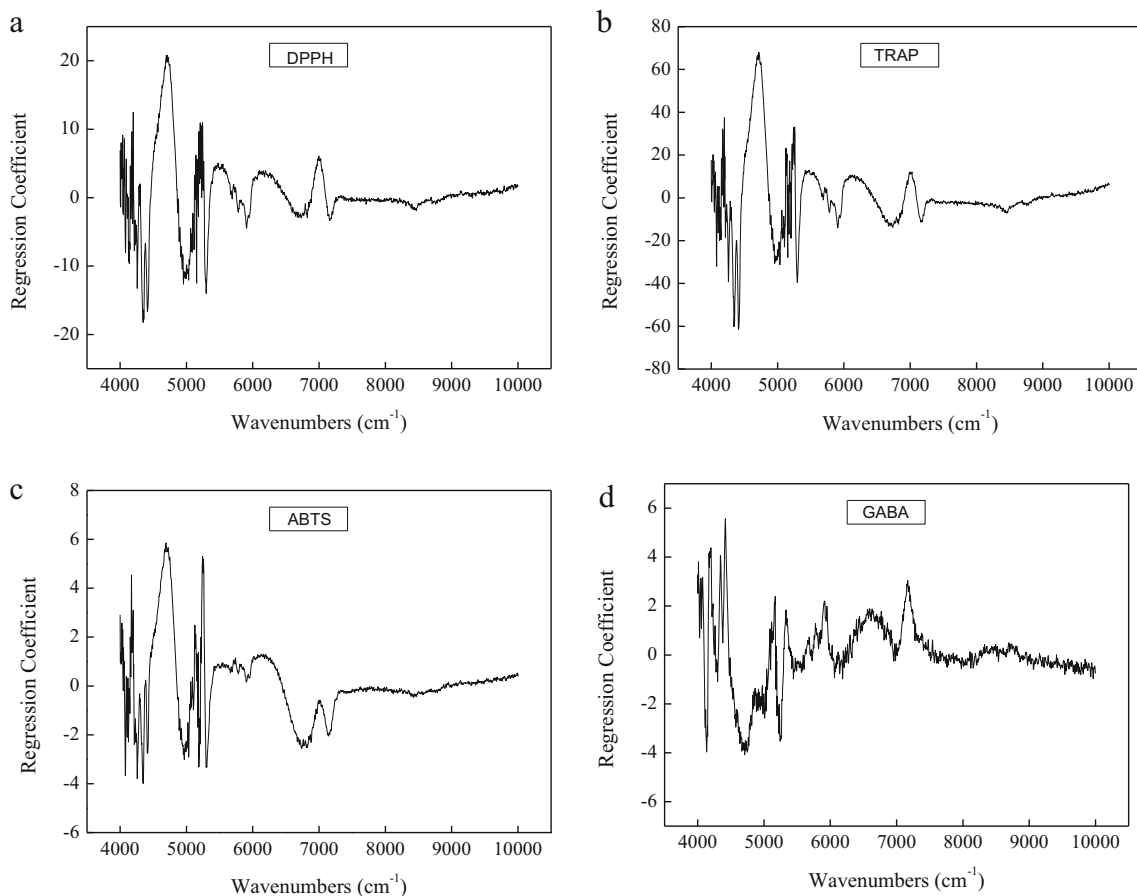
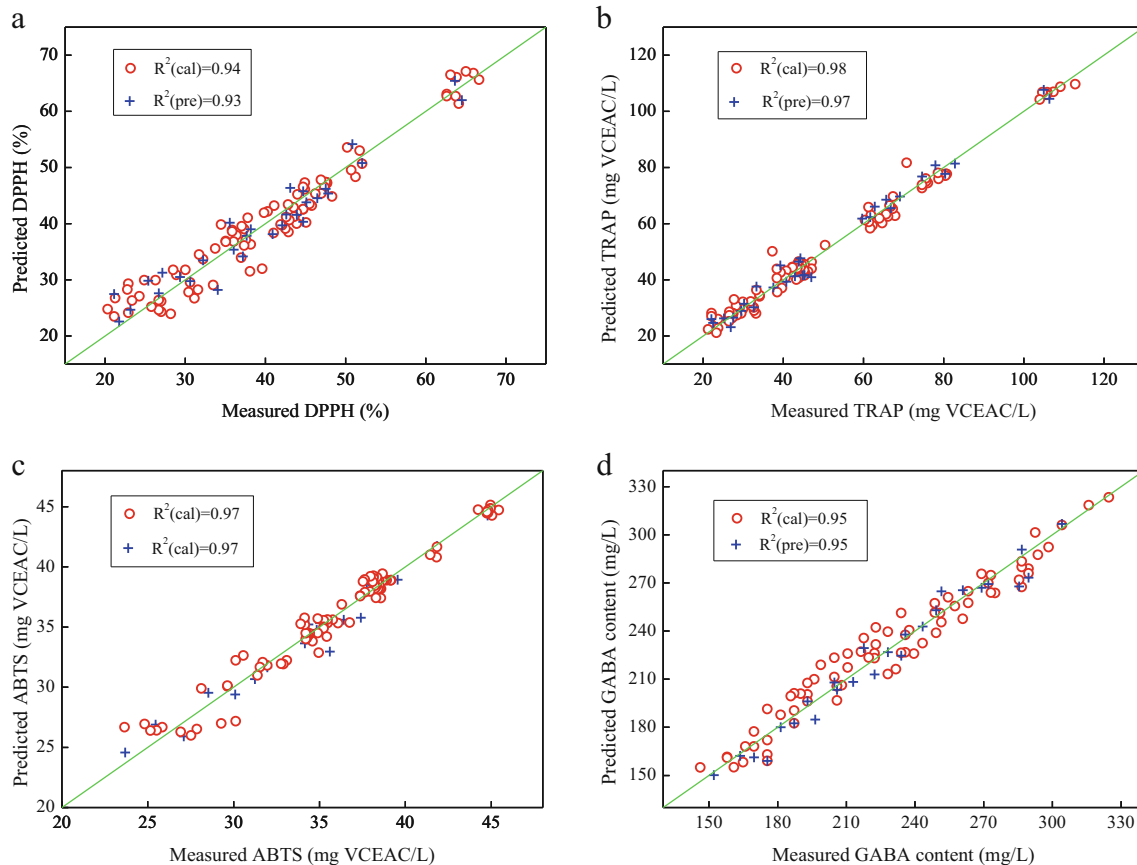
**Fig. 4** Regression coefficients obtained for PLS models of DPPH (a), TRAP (b), ABTS (c), and GABA (d)

Table 4 Results of iELM multivariate regression models based on different number of hidden layers for DPPH, ABTS, TRAP and GABA

Number of hidden layers	DPPH		ABTS		TRAP		GABA	
	R^2	RMSECV	R^2	RMSECV	R^2	RMSECV	R^2	RMSECV
5	0.234	33.83	0.158	9.24	0.091	29.05	0.522	33.22
10	0.639	21.91	0.544	2.92	0.653	16.12	0.681	25.10
15	0.863	14.46	0.811	2.31	0.829	11.38	0.920	15.62
20	0.892	11.55	0.833	2.03	0.922	9.12	0.954	8.75
25	0.940	3.07	0.972	0.79	0.892	10.19	0.943	10.41
30	0.929	5.89	0.770	2.49	0.934	7.21	0.852	19.97
35	0.932	5.74	0.892	1.44	0.926	8.97	0.929	14.46
40	0.942	2.58	0.932	1.26	0.963	5.86	0.893	18.75
45	0.931	5.81	0.937	1.15	0.982	3.55	0.933	13.70
50	0.920	6.32	0.962	0.84	0.941	6.37	0.938	11.42

results obtained from the iPLS algorithm. Therefore, the spectra variables selected by iPLS algorithm contained a lot of information related to the corresponding characteristic matters. As a result, better prediction performance established by the efficient subintervals could be better than those based on full spectrum. In addition, the iPLS

model contained only less than 90 variables, far fewer than those included in the full-spectrum PLS model (1,557 variables). The number of wavelength variables decreased by 94.22 %; thus, the iPLS model was less complex and more interpretable, at the same time, the computation time used to analysis the model was considerably shortened.

**Fig. 5** Scatter plots of reference measurements and FT-NIR predictions for DPPH (a), TRAP (b), ABTS (c), and GABA (d) by iELM models

Comparison Between the Performances of Linear Regression Models and Nonlinear Regression Models

ELM as an emergent technology has been developed for the “generalized” single-hidden layer feed-forward networks (Huang et al. 2010). Different from traditional learning algorithms for neural networks, ELM not only tends to reach the smallest training error but also the smallest norm of output weights. In ELM model, the hidden node parameters are randomly generated, the output weights can be analytically determined by using Moore-Penrose generalized inverse. The only parameter that needs to be determined is the number of hidden nodes. In this work, the number of hidden nodes was optimized in the range from 11 to 25 with an interval of 5; ELM models based on different number of hidden nodes were constructed. The optimal number of hidden nodes was according to the RMSECV values. The results of iELM models under different number of hidden nodes for DPPH, ABTS, TRAP, and GABA were shown in Table 4. The performance parameters of the optimal models of the four parameters are prominently shown in italics.

The statistics shown in Table 3 indicated that compared with iPLS models, iELM models achieved better performances on predicting the four parameters studied in this work. Among the four parameters, the predict precisions of ABTS improved the most. For regression models developed based on the NIR spectra, R^2 (pre) and RPD of ABTS increased from 0.932 and 5.27 in iPLS model to 0.970 and 6.21 in iELM model, while RMSEP (%) decreased from 2.71 to 2.30. Chinese rice wine sample was a complex system, in which a large number of chemical components existed. These chemical compounds included many chemical bonds in fundamental groups including C–H, S–H, C=O, N–H, O–H, C–O, etc.; as a result, overtones and combinations of fundamental vibrations of different chemical bonds occurred in NIR spectra. Therefore, some latent nonlinear relationship existed between NIR spectra and the fermentation parameters.

Among all the four different kinds of models (PLS, iPLS, ELM, iELM), the iELM model got the best performance with the highest R^2 (pre) and RPD and the lowest RMSEP (%). Compared with PLS models using all wavelengths of NIR spectra, R^2 (pre) of iELM models increased by 4.49, 5.43, 4.30, and 3.26 %, respectively, for DPPH, ABTS, TRAP, and GABA. The scatter plots of reference measurements and NIR predictions for the four parameters obtained from iELM models and PLS models based on full-spectral region were shown in Fig. 5. The green diagonal represents ideal results—the closer the points are to this, the better is the model. As could be seen in the plots, compared with PLS models based on the full-spectral region, iELM models based on spectral subintervals selected by iPLS algorithm had a better fitting effect between the predicted and reference data (all of the data points clustered closely to the diagonal lines).

Conclusions

The applicability of FT-NIR combined with chemometrics for the prediction of the antioxidant capacity and GABA content of Chinese rice wine was investigated. In developing calibration models, iPLS showed its incomparable superiority in contrast with classical PLS calibration method. Furthermore, ELM models performed significantly better than PLS models, indicating the correlations between the spectra and the chemical components were inclined to be nonlinear rather than linear. From all the results presented, it can be concluded that NIR together with iPLS and ELM could be utilized as alternative technique to rapidly provide information on the healthy function properties (including the antioxidant activity and GABA content) of Chinese rice wine, and has a high potential to be implemented for the rapid screening of several total antioxidant capacity assays concurrently. In the near future, for evaluating the total antioxidant capacity and GABA of CRW, firstly, with an NIR spectrometer, the spectra of a large number of CRWs from various brands and geographical origins were collected. Secondly, iPLS algorithm was used to select the most important spectral subinterval. Thirdly, the selected spectra region was input as independent X variables to build nonlinear regression models, that is iELM models. Finally, the constructed iELM model can be used to rapidly predict the total antioxidant capacity and GABA of external CRW samples.

Acknowledgments This study was supported by National ‘Twelfth Five-Year’ Plan for Science & Technology Support of China (Nos. 2012BAD37B02 and 2012BAD37B06).

Conflict of Interest Wu Zhengzong declares that he has no conflict of interest. Xu Enbo declares that he has no conflict of interest. Long Jie declares that she has no conflict of interest. Wang Fang declares that she has no conflict of interest. Jin Zhengyu declares that he has no conflict of interest. Xu Xueming declares that he has no conflict of interest. Jiao Aiquan declares that he has no conflict of interest. This article does not contain any studies with human or animal subjects.

References

- Chen Q, Ding J, Cai J, Zhao J (2012) Rapid measurement of total acid content (TAC) in vinegar using near infrared spectroscopy based on efficient variables selection algorithm and nonlinear regression tools. *Food Chem* 135(2):590–595
- de Oliveira GA, de Castilhos F, Renard CM-GC, Bureau S (2014) Comparison of NIR and MIR spectroscopic methods for determination of individual sugars, organic acids and carotenoids in passion fruit. *Food Res Int* 60:154–162
- DeFeudis FV (1983) γ -Aminobutyric acid and cardiovascular function. *Experientia* 39(8):845–849
- Fan H, Qiao Z (2000) Study for nutritional value of rice wine. *J Northwest Minorities Univ* 21(35):47–49
- Fürst P, Pollack L, Graser TA, Godel H, Stehle P (1990) Appraisal of four pre-column derivatization methods for the high-performance liquid

- chromatographic determination of free amino acids in biological materials. *J Chromatogr* 499:557–569
- Haugstad TS, Karlsen HE, Krajčič P, Due-Tønnessen B, Larsen M, Sandberg C, Sand O, Brandtzaeg P, Langmoen IA (1997) Efflux of γ -aminobutyric acid caused by changes in ion concentrations and cell swelling simulating the effect of cerebral ischaemia. *Acta Neurochir (Wien)* 139(5):453–463
- Huang G-B, Ding X, Zhou H (2010) Optimization method based extreme learning machine for classification. *Neurocomputing* 74(1–3):155–163
- Jiang H, Liu G, Mei C, Yu S, Xiao X, Ding Y (2012) Measurement of process variables in solid-state fermentation of wheat straw using FT-NIR spectroscopy and synergy interval PLS algorithm. *Spectrochim Acta A* 97:277–283
- Joye IJ, Lamberts L, Brijs K, Delcour JA (2011) In situ production of γ -aminobutyric acid in breakfast cereals. *Food Chem* 129(2):395–401
- Kim HS, Lee EJ, Lim S-T, Han J-A (2015) Self-enhancement of GABA in rice bran using various stress treatments. *Food Chem* 172:657–662
- Lan Y, Soh YC, Huang G-B (2010) Constructive hidden nodes selection of extreme learning machine for regression. *Neurocomputing* 73(16–18):3191–3199
- Li H, Jin Z, Xu X (2013) Design and optimization of an efficient enzymatic extrusion pretreatment for Chinese rice wine fermentation. *Food Control* 32(2):563–568
- Liu T, Zhou Y, Zhu Y, Song M, Li B-b, Shi Y, Gong J (2014) Study of the rapid detection of γ -aminobutyric acid in rice wine based on chemometrics using near infrared spectroscopy. *J Food Sci Tech* 1–5
- Lu X, Wang J, Al-Qadiri HM, Ross CF, Powers JR, Tang J, Rasco BA (2011) Determination of total phenolic content and antioxidant capacity of onion (*Allium cepa*) and shallot (*Allium oschaninii*) using infrared spectroscopy. *Food Chem* 129(2):637–644
- Machado M, Machado N, Gouvinhas I, Cunha M, de Almeida JMM, Barros ARNA (2014) Quantification of chemical characteristics of olive fruit and oil of cv Cobrançosa in two ripening stages using mir spectroscopy and chemometrics. *Food Anal Methods* 1–9
- Niu X, Shen F, Yu Y, Yan Z, Xu K, Yu H, Ying Y (2008) Analysis of sugars in Chinese rice wine by Fourier transform near-infrared spectroscopy with partial least-squares regression. *J Agric Food Chem* 56(16):7271–7278
- Norgaard L, Saudland A, Wagner J, Nielsen JP, Munck L, Engelsen SB (2000) Interval partial least-squares regression (iPLS): a comparative chemometric study with an example from near-infrared spectroscopy. *Appl Spectrosc* 54(5):413–419
- Ouyang Q, Chen Q, Zhao J, Lin H (2012) Determination of amino acid nitrogen in soy sauce using near infrared spectroscopy combined with characteristic variables selection and extreme learning machine. *Food Bioprocess Technol* 6(9):2486–2493
- Oyaizu M (1986) Studies on products of browning reaction—antioxidative activities of products of browning reaction prepared from glucosamine. *Jpn J Nutr* 44:307–315
- Ozgen M, Reese RN, Tulio AZ, Scheerens JC, Miller AR (2006) Modified 2,2-azino-bis-3-ethylbenzothiazoline-6-sulfonic acid (ABTS) method to measure antioxidant capacity of selected small fruits and comparison to ferric reducing antioxidant power (FRAP) and 2,2'-diphenyl-1-picrylhydrazyl (DPPH) methods. *J Agric Food Chem* 54(4):1151–1157
- Pang K, Zhang A (2011) Study on antioxidant mechanism of carnosine, alanine and histidine. *Amino Acids Biotic Resour* 33(4):33–35
- Peng J, Mao J, Huang G, Ji Z, Feng H, Zhang M (2012) Study on the antioxidant activity of polysaccharide from Chinese rice wine in vitro. *Sci Technol Food Ind* 33(20)
- Que F, Mao L, Pan X (2006a) Antioxidant activities of five Chinese rice wines and the involvement of phenolic compounds. *Food Res Int* 39(5):581–587
- Que F, Mao L, Zhu C, Xie G (2006b) Antioxidant properties of Chinese yellow wine, its concentrate and volatiles. *LWT Food Sci Technol* 39(2):111–117
- Rong H-J, Ong Y-S, Tan A-H, Zhu Z (2008) A fast pruned-extreme learning machine for classification problem. *Neurocomputing* 72(1–3):359–366
- Schonbichler SA, Falser GFJ, Hussain S, Bittner LK, Abel G, Popp M, Bonn GK, Huck CW (2014) Comparison of NIR and ATR-IR spectroscopy for the determination of the antioxidant capacity of *Primulae flos cum calycibus*. *Anal Methods* 6(16):6343–6351
- Shen F, Niu X, Yang D, Ying Y, Li B, Zhu G, Wu J (2010a) Determination of amino acids in Chinese rice wine by Fourier transform near-infrared spectroscopy. *J Agric Food Chem* 58(17):9809–9816
- Shen F, Yang D, Ying Y, Li B, Zheng Y, Jiang T (2010b) Discrimination between Shaoxing wines and other Chinese rice wines by near-infrared spectroscopy and chemometrics. *Food Bioprocess Technol* 5(2):786–795
- Shen F, Ying Y, Li B, Zheng Y, Hu J (2011) Prediction of sugars and acids in Chinese rice wine by mid-infrared spectroscopy. *Food Res Int* 44(5):1521–1527
- Shen F, Li F, Liu D, Xu H, Ying Y, Li B (2012a) Ageing status characterization of Chinese rice wines using chemical descriptors combined with multivariate data analysis. *Food Control* 25(2):458–463
- Shen F, Ying Y, Li B, Zheng Y, Liu X (2012b) Discrimination of blended Chinese rice wine ages based on near-infrared spectroscopy. *Int J Food Prop* 15(6):1262–1275
- Silva SD, Feliciano RP, Boas LV, Bronze MR (2014) Application of FTIR-ATR to Moscatel dessert wines for prediction of total phenolic and flavonoid contents and antioxidant capacity. *Food Chem* 150:489–493
- Tan S, Huo Y, Wu J, Fei P (2014) Research advance of antioxidation and corresponding ingredients of Chinese yellow wine. *Sci Technol Food Ind* 35(9):396–400
- Versari A, Parpinello GP, Scazzina F, Rio DD (2010) Prediction of total antioxidant capacity of red wine by Fourier transform infrared spectroscopy. *Food Control* 21(5):786–789
- Wu Z, Xu E, Wang F, Long J, Jiao X, Jin Z (2014) Rapid determination of process variables of Chinese rice wine using FT-NIR spectroscopy and efficient wavelengths selection methods. *Food Anal Methods* 1–12
- Wu Z, Xu E, Long J, Zhang Y, Wang F, Xu X, Jin Z, Jiao A (2015) Monitoring of fermentation process parameters of Chinese rice wine using attenuated total reflectance mid-infrared spectroscopy. *Food Control* 50:405–412
- Xie G, Dai J, Zhao G, Shuai G, Li L (2005) γ -Aminobutyric acid in the rice wine and its healthy functionwine. *China Brew* (3):49–50
- Xu E, Wu Z, Wang F, Li H, Xu X, Jin Z, Jiao A (2014) Impact of high-shear extrusion combined with enzymatic hydrolysis on rice properties and Chinese rice wine fermentation. *Food Bioprocess Technol* 1–16
- Ye J, Chen G, Ni L (2006) Study on the antioxidant activity of Fujian yellow rice wine. *J Chin Inst Food Sci Technol* 6(1):345–350
- Yu H, Zhou Y, Fu X, Xie L, Ying Y (2007) Discrimination between Chinese rice wines of different geographical origins by NIRS and AAS. *Eur Food Res Technol* 225(3–4):313–320
- Zhang K-Z, Deng K, Luo H-B, Zhou J, Wu Z-Y, Zhang W-X (2013) Antioxidant properties and phenolic profiles of four Chinese Za wines produced from hull-less barley or maize. *J Inst Brew* 119(3):182–190
- Zhang C, Xu N, Luo L, Liu F, Kong W, Feng L, He Y (2014) Detection of aspartic acid in fermented cordyceps powder using near infrared spectroscopy based on variable selection algorithms and multivariate calibration methods. *Food Bioprocess Technol* 7(2):598–604